The Plant Cell, Vol. 18, 2567–2581, October 2006, www.plantcell.org © 2006 American Society of Plant Biologists

# The Proteolytic Processing of Seed Storage Proteins in *Arabidopsis* Embryo Cells Starts in the Multivesicular Bodies [W]

**Marisa S. Otegui,[a,b,1] Rachel Herder,[a] Jan Schulze,[c] Rudolf Jung,[c] and L. Andrew Staehelin[d]**

[a] Department of Botany, University of Wisconsin, Madison, Wisconsin 53706
[b] Instituto de Fisiología Vegetal, Universidad Nacional de La Plata, 1900 La Plata, Argentina
[c] Pioneer Hi-Bred International, a Dupont Company, Johnston, Iowa 50131-1004
[d] Department of Molecular, Cellular, and Developmental Biology, University of Colorado, Boulder, Colorado 80309-0347

**We have investigated the transport of storage proteins, their processing proteases, and the Vacuolar Sorting Receptor-1/Epidermal Growth Factor Receptor–Like Protein1 (VSR-1/ATELP1) receptor during the formation of protein storage vacuoles in *Arabidopsis thaliana* embryos by means of high-pressure freezing/freeze substitution, electron tomography, immunolabeling techniques, and subcellular fractionation. The storage proteins and their processing proteases are segregated from each other within the Golgi cisternae and packaged into separate vesicles. The storage protein–containing vesicles but not the processing enzyme–containing vesicles carry the VSR-1/ATELP1 receptor. Both types of secretory vesicles appear to fuse into a type of prevacuolar multivesicular body (MVB). We have also determined that the proteolytic processing of the 2S albumins starts in the MVBs. We hypothesize that the compartmentalized processing of storage proteins in the MVBs may allow for the sequential activation of processing proteases as the MVB lumen gradually acidifies.**

## INTRODUCTION

Seeds contain large amounts of different types of seed storage proteins, which serve as the primary source of reduced nitrogen for the growing seedling during germination. In developing dicot seeds, the most abundantly expressed storage proteins are members of the 2S albumin and the 7S and 11S globulin protein families. Precursor polypeptides of these storage protein classes are synthesized at the endoplasmic reticulum (ER), and the mature (processed) polypeptides of all of these three protein classes accumulate inside specialized vacuoles, called protein storage vacuoles (PSVs) (Muntz, 1998; Robinson and Hinz, 1999; Holkeri and Vitale, 2001; Jiang et al., 2001).

At least three different pathways have been recognized for the trafficking of storage proteins from the ER to the PSV: the Golgi-dependent dense vesicle pathway; the direct ER-to-PSV transport pathway; and the autophagic pathway. Although the Golgi pathway is considered the most prominent trafficking route in most systems, the prevalence of each of these pathways depends on the plant species, the tissue type, the developmental stage, the physiological status of the cell, and the storage protein class (Robinson et al., 2005). In legumes, globulin storage proteins traffic through the Golgi, where they form aggregates in specialized marginal buds of the *cis*-Golgi cisternae that progress through the stack (Hillmer et al., 2001) as the cisternae mature. Upon reaching the *trans*-Golgi network (TGN), the buds with the protein aggregates give rise to electron-dense vesicles, which lack a distinct coat (Hillmer et al., 2001; Robinson et al., 2005; Vitale and Hinz, 2005). The dense vesicles fuse with multivesicular bodies (MVBs), which deliver their contents to the PSVs (Robinson et al., 1998, 2005; Vitale and Hinz, 2005). In pea (*Pisum sativum*), the dense vesicles measure 150 nm in diameter and exhibit an electron-lucent peripheral layer enriched in sucrose binding protein, a minor 7S globulin homologue (Wenzel et al., 2005), and a dense central core containing the two major pea storage proteins, the 7S globulin vicilin and the 11S globulin legumin (Hohl et al., 1996).

Although most of the structural and biochemical studies of dense vesicles have focused on legumes (Greenwood and Chrispeels, 1985; Hinz et al., 1999; Robinson and Hinz, 1999; Hillmer et al., 2001), similar electron-dense buds attached to the Golgi have been observed previously in *Arabidopsis thaliana* embryo cells (Mansfield and Briarty, 1992). The formation of dense vesicles seems to require both protein aggregation and receptor-mediated sorting (Shimada et al., 2003a; Wenzel et al., 2005). A recent report indicates that the *Arabidopsis* Vacuolar Sorting Receptor-1/Epidermal Growth Factor Receptor–Like Protein1 (VSR-1/ATELP1) receptor, which sorts vacuolar proteins such as aleurain and sporamin to the plant lytic vacuole (Ahmed et al., 2000) and localizes to the prevacuolar compartment (Sanderfoot et al., 1998), also mediates the transport of both 2S albumin and 12S globulin precursors to the PSV in *Arabidopsis* (Shimada et al., 2003a).

It has been postulated that the proteases involved in storage protein processing in pea are sorted into clathrin-coated vesicles in the TGN for transport to the PSV. This hypothesis is based on the detection of BP-80, another member of the VSR/ATELP receptor family (Hinz et al., 1999), in clathrin-coated vesicles. However, because of the apparent dual role of these receptors in

[1] To whom correspondence should be addressed. E-mail otegui@wisc.edu; fax 608-262-7509.
The author responsible for distribution of materials integral to the findings presented in this article in accordance with the policy described in the Instructions for Authors (www.plantcell.org) is: Marisa S. Otegui (otegui@wisc.edu).
[W] Online version contains Web-only data.
www.plantcell.org/cgi/doi/10.1105/tpc.106.040931

the sorting of both proteases and storage proteins, a positive identification of cargo molecules in the clathrin-coated vesicles in PSV-forming cells has yet to be reported.

In *Arabidopsis*, the PSV formation pathway appears to be very similar to the equivalent pathway in legumes. The *Arabidopsis* PSVs contain 2S albumins and 12S globulins, proteolytic processing enzymes, such as vacuolar processing enzymes (VPEs) and the aspartic protease A1, as well as phytic acid crystals called globoids (da Silva Conceicao and Krebbers, 1994; Mutlu et al., 1999; Chen et al., 2002; Gruis et al., 2002; Otegui et al., 2002). The *Arabidopsis* 2S albumins are exported from the ER as precursors that contain three propeptides (an N-terminal propeptide, an internal propeptide, and a C-terminal propeptide). These propeptides are removed posttranslationally by proteolytic processing enzymes (Gruis et al., 2002, 2004; Shimada et al., 2003b).

Transport of the storage proteins from the TGN to the PSVs in legumes occurs via MVB compartments, which act as prevacuolar compartments, as indicated by immunogold localization experiments (Robinson et al., 1998; Robinson and Hinz, 1999). In mammalian cells, endocytic tracers destined for degradation are segregated from recycling receptors as they traffic through the MVBs and before they reach the lysosomes (Geuze et al., 1983). For this reason, MVBs are also referred to as multivesicular endosomes (Gruenberg and Stenmark, 2004). One of the common functional properties of MVBs is their ability to invaginate membrane domains containing membrane proteins destined for degradation in lysosomes/lytic vacuoles (Katzmann et al., 2002). In addition to their function in the endocytic pathway, MVBs also traffic secretory cargo from the Golgi to the lysosomes/vacuoles, allowing for the recycling of receptors such as the mammalian mannose-6-phosphate receptor (Griffiths et al., 1988) or the plant BP-80 receptor back to the Golgi/TGN (daSilva et al., 2005).

The study of plant MVB functions is challenging because many plant cells, including legume embryo cells, contain two types of vacuoles, the lytic vacuoles and the PSVs, with storage functions (Robinson and Hinz, 1999). To further understand the function of MVBs in storage protein trafficking in the *Arabidopsis* embryo, we used a combination of structural and biochemical techniques. We demonstrate that storage proteins and processing proteases are sorted at the Golgi apparatus into at least two types of vesicles, which appear to fuse with each other and give rise to MVBs. Interestingly, the storage protein–containing vesicles but not the processing enzyme–containing vesicles carry the VSR-1/ATELP1 receptor. We also report that the initial proteolytic processing of 2S albumins, which has critical consequences for protein solubility, occurs inside these MVB compartments before the storage proteins reach the PSV. In addition, we show that during storage protein accumulation *Arabidopsis* embryo cells contain only one type of vacuole, the PSVs.

## RESULTS

### The Golgi Apparatus Produces at Least Two Types of Vesicles during the Formation of PSVs

To determine the structure and spatial organization of the secretory pathway in *Arabidopsis* embryo cells during PSV formation, we analyzed semithick sections of high-pressure frozen/freeze-substituted bent-cotyledon and late bent-cotyledon embryos by electron tomography. In these cells, Golgi stacks tend to aggregate in clusters of three to five stacks, with their *trans* sides facing each other (Figure 1A). Each cluster of Golgi stacks delimits an area in which the TGNs are very close to each other and intermixed with a high number of vesicles and MVBs (Figures 1A to 1D).

The individual Golgi stacks consist of five or six cisternae and a TGN (Figure 2). Based on structural and staining criteria (Staehelin et al., 1990), the Golgi stack shown in Figure 2 consists of two *cis* cisternae, three medial cisternae, one *trans* cisterna, and a TGN partially detached from the stack. Electron-dense aggregates were confined to the cisternal margins except in the immature *cis*-most cisterna (Figure 2C). Single and double immunogold labeling on plastic sections of late bent-cotyledon embryos demonstrates that these aggregates consist of both 12S globulins and 2S albumins (Figures 3A to 3C; see Supplemental Figure 1B online). The antibodies used for these experiments recognized either the large chain of the 2S albumins (Scarafoni et al., 2001) or epitopes on the α- and β-subunits of

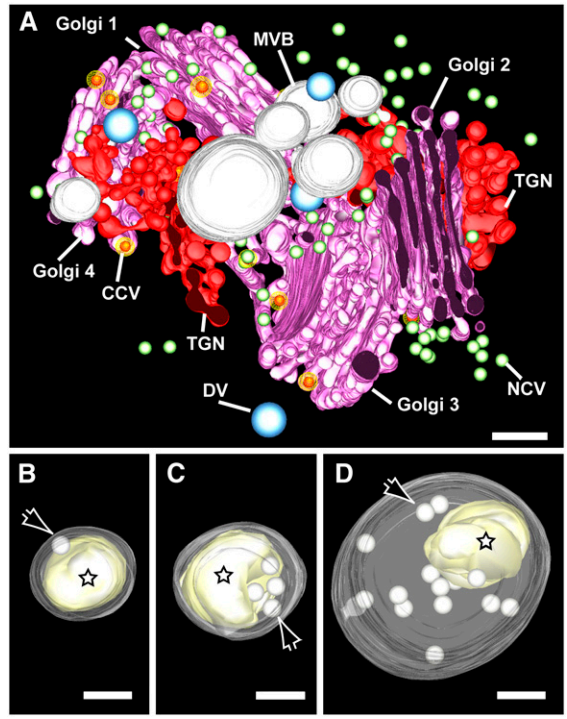


**Figure 1.** Tomographic Models of Golgi Stacks, Associated Vesicles, and Secretory Compartments during PSV Formation in the *Arabidopsis* Embryo Reconstructed from a Serial Tomogram Consisting of Five Sections.

**(A)** A cluster of four Golgi stacks delimits an area with high concentrations of TGNs, dense vesicles (DV), clathrin-coated vesicles (CCV), noncoated vesicles (NCV), and MVBs. Bar = 200 nm.

**(B)** to **(D)** MVB compartments. The limiting membranes of MVBs have been made translucent in these tomographic models to visualize the internal vesicles (arrows) and electron-dense aggregates (stars). Bars = 100 nm.

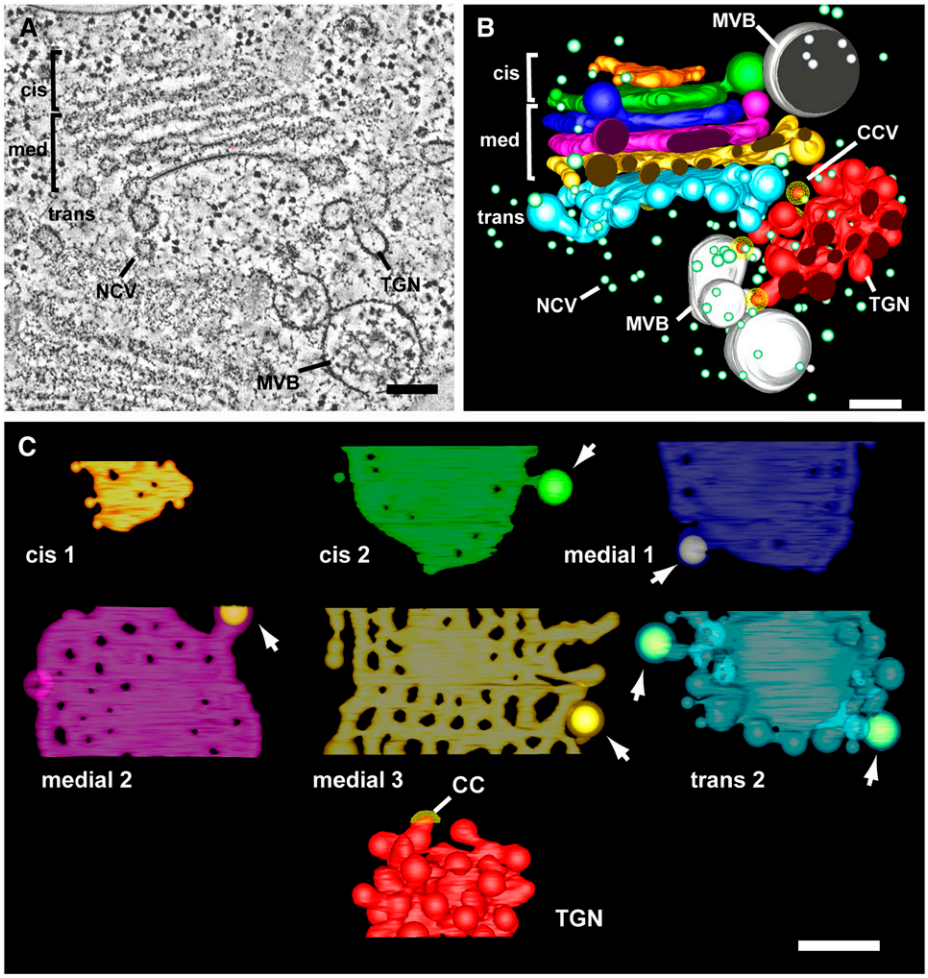


**Figure 2.** Golgi Stacks and Associated Compartments during the Formation of PSVs.

**(A)** Tomographic slice (4.3 nm thick) through a Golgi stack and associated vesicles and MVBs.
**(B)** Tomographic model derived from the tomogram depicted in **(A)**. Based on structural and staining patterns, this Golgi stack appears to consist of two *cis*-cisternae, three medial cisternae, one *trans*-cisterna, and a partially detached TGN.
**(C)** Face-on views of Golgi cisternae. Storage protein aggregates accumulate in the margins of all cisternae (arrows) except the *cis*-most cisterna. CC, clathrin coat.
Bars = 100 nm.

the 12S globulins (Shimada et al., 2003b), both in the precursors and in the mature forms. These aggregates do not change in size across the stack, suggesting that most of the sorting/aggregation is completed in the second *cis* cisterna (Figure 2C). At the TGN, only a few cisternal buds with storage protein aggregates were detected, suggesting that dense vesicles bud off either from this compartment or possibly from the *trans*-most Golgi cisterna. The TGN compartment also showed varying numbers of clathrin-coated buds (Figure 2C). In addition, the dense aggregates in the cisternal margins, the TGN, and the free dense vesicles were also labeled with antibodies against the VSR-1/ATELP1 receptor (Figures 3D to 3H; see Supplemental Figure 1D online), which has been suggested to interact with the *Arabidopsis* 2S albumin and 12S globulin storage proteins (Shimada et al., 2003a).

The vesicle-budding profiles observed in the reconstructed Golgi stacks and TGNs suggest that the *trans*-Golgi and TGN compartments produce three types of vesicles: 130-nm dense vesicles containing aggregates of storage proteins, 30- to 40-nm clathrin-coated vesicles with unknown contents (Figure 1A), and 30- to 40-nm vesicles without a detectable coat, some of which may be related to the clathrin-coated vesicles (Figures 1A and 2B).

Double immunolabeling of aspartic protease A1, a seed aspartic protease (Mutlu et al., 1999; Chen et al., 2002), and the 2S albumins showed a spatial segregation of the two secretory cargoes at the Golgi. Whereas most of the 2S albumins are concentrated in buds in the cisternal margins, aspartic protease A1 appears to localize to the central part of the Golgi cisternae and the budding profiles of the TGN (Figures 3I and 3J). The detection of the processing protease β-VPE (Gruis et al., 2004)

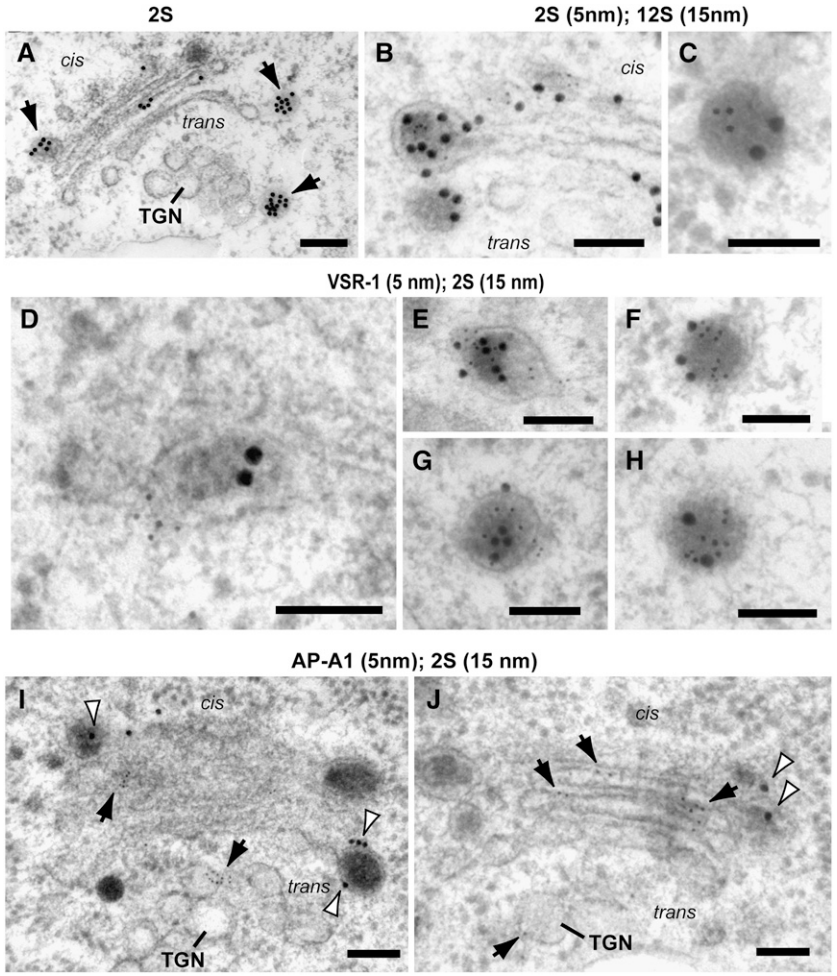


**Figure 3.** Distribution of Storage Proteins, Processing Proteases, and the VSR-1/ATELP1 Receptor in the Golgi Stacks and Dense Vesicles.

**(A)** Immunolabeling of storage proteins with anti-2S albumin antibodies. Note the high concentration of gold particles over the marginal electron-dense aggregates of the Golgi cisternae (arrows).
**(B)** and **(C)** Double immunolabeling with anti-2S albumin antibodies (5-nm gold particles) and anti-12S globulin antibodies (15-nm gold particles).
**(D)** to **(H)** Double immunolabeling of marginal buds in Golgi cisternae (**[D]** and **[E]**) and dense vesicles (**[F]** to **[H]**) with anti-VSR-1/ATELP1 antibodies (5-nm gold particles) and anti-2S albumin antibodies (15-nm gold particles).
**(I)** and **(J)** Double immunolabeling of Golgi stacks with anti-aspartic protease A1 antibodies (AtAP; 5-nm gold particles; arrows) and anti-2S albumin antibodies (15-nm gold particles; arrowheads).
Bars = 100 nm.

on plastic sections was more problematic because of the low detection signal. Nevertheless, although few gold particles were detected when the anti-β-VPE antibodies were used, we are confident about the localization pattern observed because the gold particles consistently labeled the same subcellular structures and the background labeling was very low (0.2 ± 0.1 gold particles/$\mu m^2$). On Golgi stacks, the anti-β-VPE antibodies labeled the central part of the Golgi cisternae but not the marginal aggregates (Figure 4A). We could not detect immunogold labeling of processing proteases in clathrin-coated vesicles or in any other type of vesicles located in the vicinity of the Golgi stacks. However, the absence of labeling on the clathrin-coated and noncoated vesicles may be attributable to their small size (30 to 40 nm) and the resulting limited number of molecules available for labeling in each vesicle.

### Subcellular Fractionation Experiments with *Brassica napus* Embryos Support the Sorting of Storage Proteins and Proteases into Different Types of Vesicles

Because the small size of the clathrin-coated and noncoated small vesicles might have precluded us from determining their contents by immunogold labeling, we performed subcellular fractionation of secretory vesicles from developing (late bent cotyledon) *Brassica napus* embryos. We used *B. napus* for the subcellular fractionation because it has larger embryos than

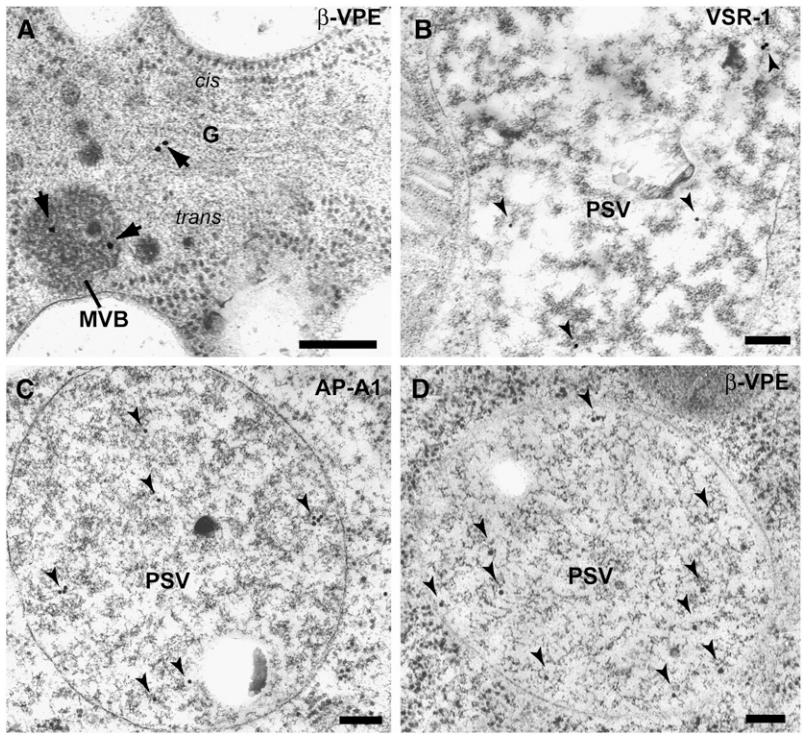


**Figure 4.** Immunolabeling of Golgi Stacks and PSVs in the *Arabidopsis* Embryo.

**(A)** Golgi stack (G) and MVB labeled with anti-β-VPE antibodies (arrows).
**(B)** PSV labeled with anti-VSR-1 antibodies (arrowheads).
**(C)** PSV labeled with anti-aspartic protease A1 antibodies (AtAP; arrowheads).
**(D)** PSV labeled with anti-β-VPE antibodies (arrowheads).
Bars = 100 nm.

*Arabidopsis* and both species show a high degree of conservation at the protein sequence level. The subcellular fractionation method was based on a protocol developed by Hinz et al. (1999) and consisted of a combination of step and rate-zonal sucrose density gradients (Figure 5). Vesicles were first enriched by centrifugation in step sucrose gradients and subsequently fractionated by centrifugation in a continuous 20 to 55% sucrose gradient (rate-zonal gradient).

Based on immunoblotting, fractions 1 to 3 from the rate-zonal gradient were highly enriched in vesicles containing 2S albumin precursors and the VSR-1/ATELP1 receptor, whereas fraction 4 contained vesicles with the β-VPE and aspartic protease A1 processing enzymes (Figure 5). These results, together with the structural tomographic analysis, indicate that the seed storage proteins (2S albumins and 12S globulins) and their processing proteases are sorted into different types of vesicles. No bands corresponding to clathrin were detected in any vesicle fraction when the membranes were incubated with a monoclonal anti-clathrin heavy chain antibody (data not shown). This is not entirely surprising considering that, in the past, it has only been possible to detect clathrin in vesicle fractions of pea embryos after collecting large amounts of cotyledons for the fractionation experiments (Hinz et al., 1999). The smaller size of the *B. napus* embryos makes it nearly impossible to collect comparable amounts of starting material.

In the pellet fraction of the 2500*g* centrifugation step, which, based on the abundance of the processed form of the 2S albumin (Figure 5, see immunodetection of the 2S albumin large chain) appears to contain the PSVs, the anti-VSR-1/ATELP1 antibody recognized two bands, one that corresponds to the receptor (~80 kD) and the other, also reported by Shimada et al. (2003a), that probably corresponds to a degradation product (Figure 5). In agreement with this observation, the anti-VSR-1/ATELP1 antibody labeled the vacuolar lumen of PSVs on plastic sections but not their tonoplast (Figure 4B).

To determine the purity of the fractions, we also tested the fractions with antibodies against well-characterized subcellular markers: *Arabidopsis* $Ca^{2+}$-ATPase2 (ACA2) for the ER (Hwang et al., 2000), α-mannosidase (α-man) for the Golgi (Preuss et al., 2004), and *Arabidopsis* UBX Domain–containing Protein1 (PUX1) for the cytoplasm (Rancour et al., 2004) (Figure 5).

### MVBs Associated with Golgi Stacks Contain Both Storage Proteins and Processing Proteases

Upon demonstrating that storage proteins and proteases were sorted into different types of vesicles, we determined the composition of the contents of the MVBs associated with the Golgi stacks. These MVBs contain dense protein aggregates that were labeled with antibodies raised against both the 2S albumin and

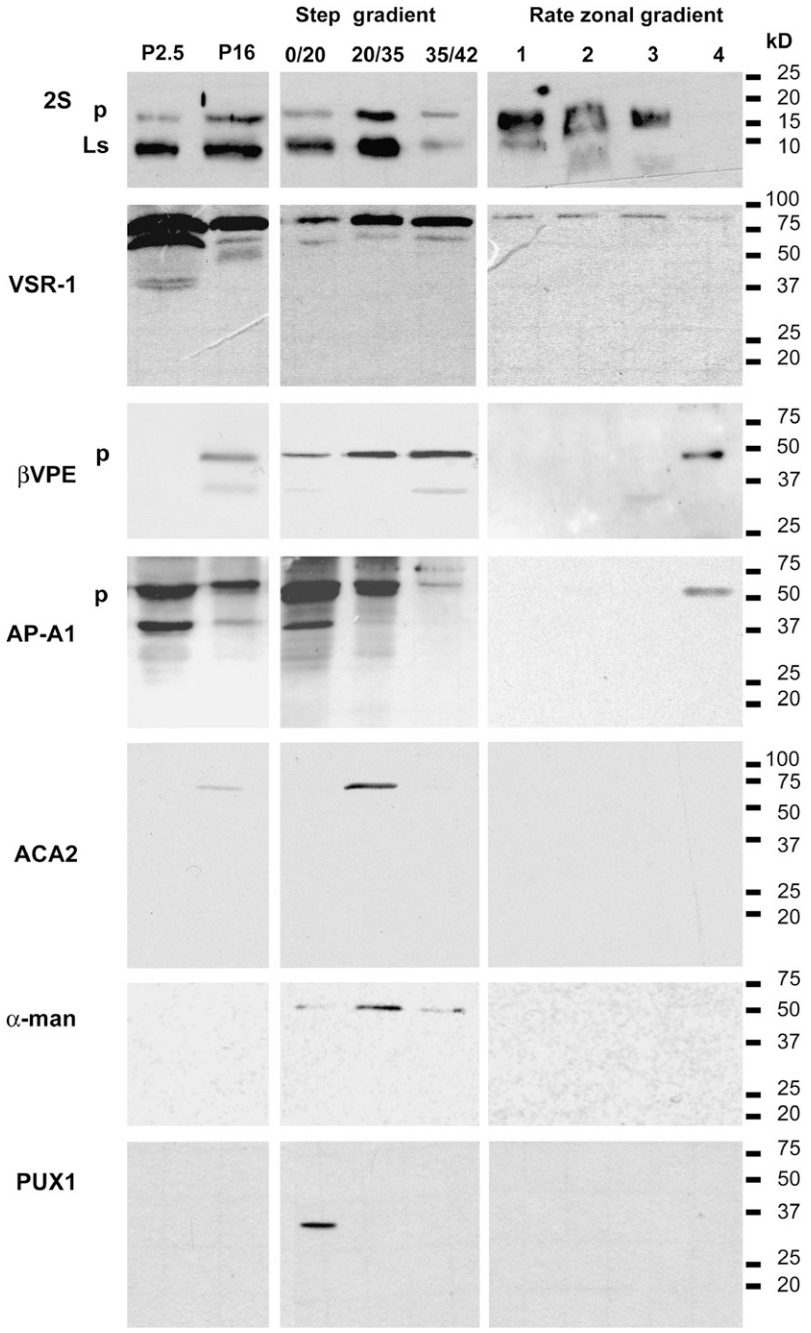


**Figure 5.** Protein Gel Blot Analysis of the Subcellular Fractions from *B. napus* Embryos.

P2.5 and P16 are the pellet fractions collected after the 2,500*g* and 16,000*g* centrifugation steps, respectively. The 16,000*g* supernatant was applied onto a sucrose density step gradient (20, 35, 42, and 55% [w/v] sucrose) and centrifuged at 85,500*g* for 120 min. The 42 to 55% sucrose interphase, which is enriched in secretory vesicles (Hinz et al., 1999), was layered onto a linear sucrose density gradient (20 to 55% sucrose) and centrifuged at 16,000*g* for 20 min (rate-zonal gradient). The rate-zonal gradient fractions 1 to 4 were collected from the top of the tube. Fractions 1 (22% sucrose) to 3 (28% sucrose) contain the 2S albumin precursors and the VSR-1/ATELP1 receptor but not the processing enzymes β-VPE and aspartic protease A1 (AtAP), whereas fraction 4 (31% sucrose) contains the processing enzyme precursors but not the storage proteins. Antibodies against subcellular markers were used to ensure the purity of the fractions: *Arabidopsis* $Ca^{2+}$-ATPase2 (ACA2) for the ER, α-mannosidase (α-man) for the Golgi, and *Arabidopsis* UBX Domain–containing Protein1 (PUX1) for the cytoplasm. Ls, 2S albumin large subunit; p, precursor.

the 12S globulin storage proteins (Figures 6A to 6C). Interestingly, the β-VPE and aspartic protease A1 processing proteases were also detected inside the MVBs (Figures 6D and 6E). We further confirmed the occurrence of storage proteins and aspartic protease A1 in the same MVBs by double immunolabeling (Figure 6F). This finding suggests that the electron-dense vesicles carrying the storage proteins and the vesicles containing the processing enzymes fuse with the same MVB compartment. In addition, we have detected the receptor VSR-1/ATELP1 in the limiting membrane and internal vesicles of these storage protein–containing MVBs (Figures 6G to 6I).

The 2S albumins and 12S globulins and the β-VPE and aspartic protease A1 processing proteases have also all been detected in the lumen of PSVs (Figures 4C and 4D; see Supplemental Figures 1A and 1B online). Because both lytic vacuoles and PSVs have been postulated to coexist in legume embryo cells, we also tried to identify lytic vacuoles in *Arabidopsis* embryo cells. We used antibodies against radish TIP-VM23 (Maeshima, 1992), which is a member of the γ-TIP subfamily of aquaporins and a marker for lytic vacuoles (Paris et al., 1996; Otegui et al., 2005). In ~100 analyzed cells from the late bent-cotyledon and mature embryo stages, no γ-TIP–positive vacuoles were detected (data not shown), whereas all identified vacuolar compartments contained storage proteins, suggesting that only PSVs occur in embryo cells at these stages of development.

### Proteolytic Processing of 2S Albumins Starts in the Secretory MVBs

The presence of the processing enzymes and their storage protein substrates in MVBs suggests that the proteolytic processing of the 2S albumins and 12S globulins could start at the prevacuolar compartments, before reaching the PSVs. To test this hypothesis, we raised antibodies against the N-terminal (N-PP) and the internal (I-PP) propeptides (Figure 7A) of an *Arabidopsis* 2S albumin precursor. These propeptides are removed during processing of the 2S albumin precursors; therefore, the loss of the epitopes is an indication that proteolytic processing has already occurred.

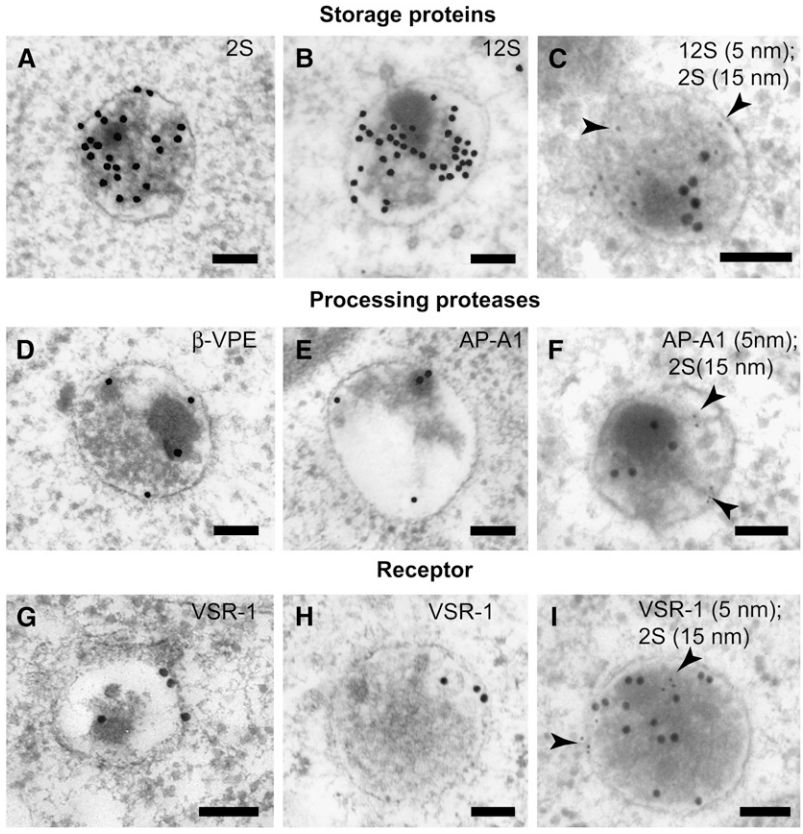


**Figure 6.** Immunolabeling of MVBs during PSV Formation in *Arabidopsis* Embryo Cells.

**(A)** to **(C)** Antibodies against storage proteins. Single immunolabeling of 2S albumins **(A)** and 12S globulins **(B)**, and double immunolabeling of 2S albumins (15-nm gold particles) and 12S globulins (5-nm gold particles) **(C)**.
**(D)** and **(E)** Antibodies against proteolytic processing enzymes: anti-β-VPE **(D)** and anti-aspartic protease A1 (AtAP) **(E)** antibodies.
**(F)** Double immunolabeling of aspartic protease A1 (5-nm gold particles) and 2S albumins (15-nm gold particles).
**(G)** and **(H)** Antibodies against the VSR-1/ATELP1 receptor.
**(I)** Double immunolabeling of the VSR-1/ATELP1 receptor (5-nm gold particles) and 2S albumins (15-nm gold particles).
Bars = 100 nm.

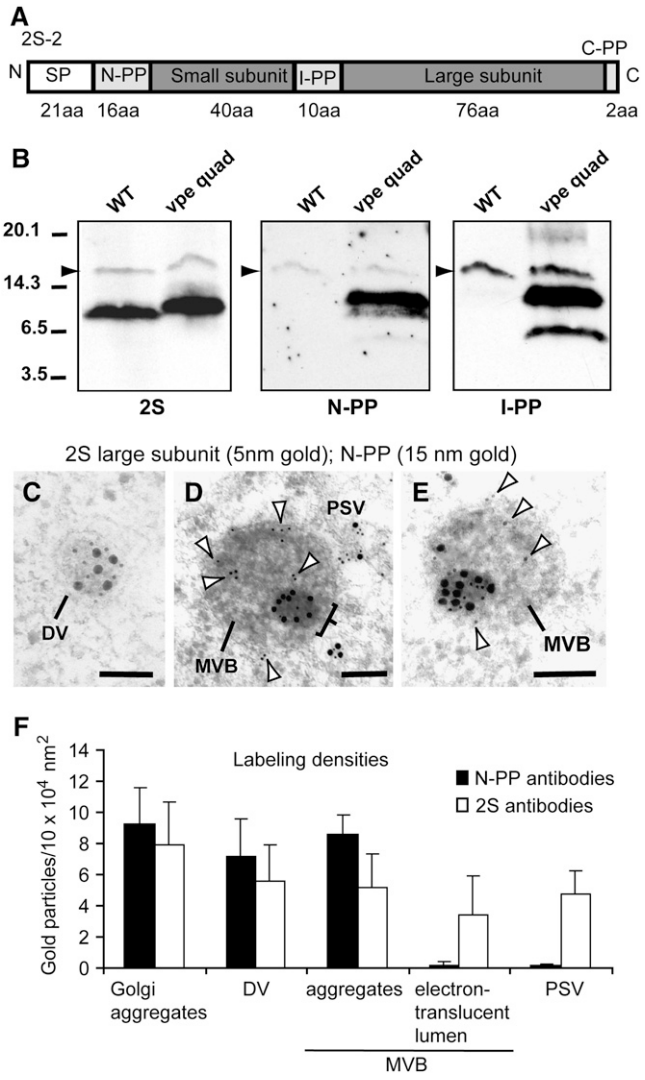


**Figure 7.** Detection of 2S Albumin Propeptides.

**(A)** Diagram of an *Arabidopsis* 2S albumin precursor: signal peptide (SP), three propeptides (N-terminal propeptide [N-PP], internal propeptide [I-PP], and C-terminal propeptide [C-PP]), and the small and large chains. aa, amino acids.

**(B)** Protein gel blots of protein extracts from both wild-type and *vpe*-quadruple mutant *Arabidopsis* seeds. The anti-2S albumin antibodies (2S) recognize the 2S albumin large chain in both the precursor (~15 kD) and the mature (~7 kD) forms; the I-PP peptide antibodies recognize the 2S albumin internal propeptide; and the N-PP peptide antibodies recognize the 2S albumin N-terminal propeptide. Arrowheads indicate the 2S albumin precursors.

**(C)** to **(E)** Double immunolabeling of a dense vesicle **(C)** and MVBs (**[D]** and **[E]**) with anti-2S albumin antibodies (5-nm gold particles) and anti-N-PP antibodies (15-nm gold particles). The less electron-dense luminal contents that surround the dense aggregate inside MVBs are labeled with anti-2S albumin antibodies (arrowheads) but are very scarcely labeled with anti-N-PP antibodies. Bars = 100 nm.

**(F)** Labeling density on different organelles with the N-PP and 2S albumin antibodies. Values shown are means of 10 to 15 sampled areas, and error bars indicate SE.

The two peptide antibodies were tested by immunoblot analysis of protein extracts from developing *Arabidopsis* wild-type seeds (bent-cotyledon embryo stage). A weak band of ~15 kD, which corresponds in size to 2S albumin precursors, was detected with the anti-I-PP antibody. A band of a similar size, although fainter, was also detected with the anti-N-PP antibody (Figure 7B). We consequently concluded that both propeptide antibodies are able to specifically recognize the small pool of unprocessed 2S albumin precursors en route to processing sites and do not cross-react with the mature 2S albumin chains or with any other *Arabidopsis* seed proteins in immature wild-type seeds. The putative 2S albumin precursor band was not detected by the propeptide antibodies in protein extracts from mature seeds (data not shown), in agreement with earlier reports (Gruis et al., 2004).

To provide an unambiguous control for the specificity of the N-PP and I-PP antibodies, we then tested these antibodies on seed protein extracts from the *Arabidopsis vpe*-quadruple mutant (Gruis et al., 2004), which lacks all four members (α-VPE, β-VPE, γ-VPE, and δ-VPE) of the VPE family and fails to fully process the 2S albumin precursors (Shimada et al., 2003b; Gruis et al., 2004). In the *vpe*-quadruple mutant protein extracts, the propeptide antibodies strongly labeled several bands between 15 and 6 kD (Figure 7B), which correspond to precursors and to alternatively processed 2S albumin polypeptides (Gruis et al., 2004). In alternatively processed 2S albumin polypeptides, ~50% of the N-PP amino acid sequence and ~30% of the I-PP amino acid sequence are removed (Gruis et al., 2004). Therefore, the prominent labeling of these alternatively processed polypeptides using anti-N-PP and anti-I-PP antisera indicated efficient binding of the specific immunoglobulins to epitopes in portions of the propeptides that remained attached to the alternatively processed albumin chains. As shown in Supplemental Figure 2 online, intense labeling with the antibodies against the two propeptides was detected on PSVs from the *vpe*-quadruple mutant, whereas the labeling was very low in PSVs of wild-type embryo cells. Together, these results further confirm that in the wild type, the peptide antibodies only recognize the propeptides in the 2S albumin precursors but do not cross-react with the 2S albumin mature forms.

Using these antibodies, we performed double immunolabeling experiments on sections of wild-type developing seeds to determine in which cellular compartments the processing of the 2S albumins occurs. In the Golgi marginal aggregates and the free dense vesicles, the anti-2S albumin antibody labeling (5-nm gold particles) and the anti-N-PP antibody labeling (15-nm gold particles) fully colocalize, indicating that the electron-dense vesicles carry only storage protein precursors (Figure 7C). However, in the MVBs, the anti-N-PP antibodies, which recognize only the precursor protein, labeled only the dense aggregates shown in Figures 1B to 1D but not the more lightly stained material surrounding the dense aggregates. By contrast, the anti-2S albumin antibodies, which also recognize the processed protein, also labeled the surrounding lightly stained luminal contents (Figures 7D and 7E). Similar results were obtained with the I-PP antibodies (see Supplemental Figure 1C online). This differential immunolabeling pattern indicates that the electron-dense aggregates inside MVBs contain the 2S albumin precursors, whereas the

less dense luminal contents that surround the dense aggregates are composed mostly of the processed form of the 2S albumin storage proteins. These results strongly indicate that the initial processing of the 2S albumins during embryo development occurs in the MVBs.

### Transformation of Dense Vesicles into MVBs Appears to Involve Fusion with Smaller Vesicles

The storage protein–containing compartments found in close proximity to Golgi stacks vary in size (150 to 500 nm in diameter) and morphology. Whereas all of them contain electron-dense aggregates of storage proteins, the aggregates become smaller and more dispersed as these compartments increase in size and accumulate internal vesicles (Figures 8A to 8F). We have found a number of intermediate structures that suggest that the large MVBs arise at least partially from the fusion of dense vesicles with smaller (30 to 40 nm in diameter) vesicles (Figures 8B and 8E). Most likely, these small vesicles deliver the processing proteases to the large dense vesicles and, as the resulting compartments enlarge, they start to invaginate portions of the limiting membrane that give rise to the internal vesicles of MVBs (Figures 8C and 8F).

By calculating the surface areas of prevacuolar compartments at different stages of maturation, we have identified a linear correlation between limiting membrane surface area and the number of internal vesicles (Figure 8G). Furthermore, our analysis indicates that these compartments start to develop internal

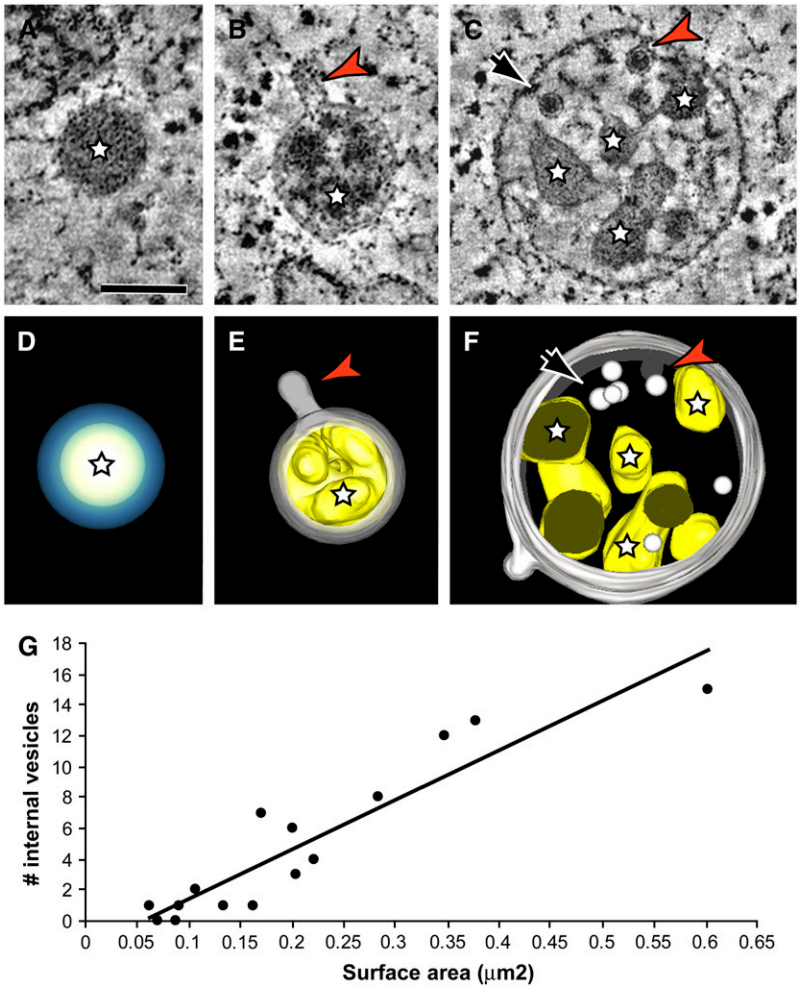


**Figure 8.** Formation of MVBs.

**(A)** to **(C)** Tomographic slices of an electron-dense vesicle **(A)**, a putative intermediate pre-MVB compartment **(B)**, and an MVB **(C)** in *Arabidopsis* embryo cells. Bar = 100 nm.

**(D)** to **(F)** Three-dimensional tomographic models corresponding to the structures depicted in **(A)** to **(C)**, respectively. The electron-dense aggregates of storage proteins are indicated by stars. The putative pre-MVB depicted in **(B)** and **(E)** shows a vesicle-budding/fusing profile (arrowheads). The MVB depicted in **(C)** and **(F)** shows a forming internal vesicle invaginating from the limiting membrane (arrowheads) and numerous internal vesicles (arrows).

**(G)** Relationship between the surface area of MVBs and the number of internal vesicles. Surface area and number of internal vesicles were calculated for 25 intermediate and MVB compartments using IMOD software.

vesicles once they surpass a membrane surface area threshold of ~0.075 $\mu m^2$.

### The pH inside the PSV Acidifies during Storage Protein Deposition

To better understand the environment inside the PSVs and how the proteolytic activity may be regulated in this compartment, we measured the luminal pH of PSVs during development. We used the acidotropic fluorescent probe Lysosensor Yellow/Blue DND-160, which has been shown to be sequestered into vacuolar compartments (Swanson et al., 1998; Otegui et al., 2005) and to exhibit both dual-excitation and dual-emission spectral peaks that are pH-dependent (Diwu et al., 1999).

Once the calibration curve was calculated (Figure 9A), we measured the intensity ratio ($I_{340/380}$) in PSVs of embryos at different stages of development (torpedo, bent-cotyledon, late bent-cotyledon, and mature embryos) (Figure 9B). The luminal pH of the PSVs decreases from 6.1 ± 0.8 in the late torpedo stage to 4.9 ± 0.1 in the mature embryo. By immunolabeling, we started to detect the accumulation of storage proteins inside PSVs at the bent-cotyledon stage. Based on these correlative data, we conclude that the pH inside the PSVs varies between ~5.5 and ~4.9 during storage protein deposition. When this pH range is superimposed on the solubility curve of the mature forms of the 12S globulins (Gruis et al., 2004), it is seen that these proteins should remain largely insoluble inside the developing PSV (Figure 9B).

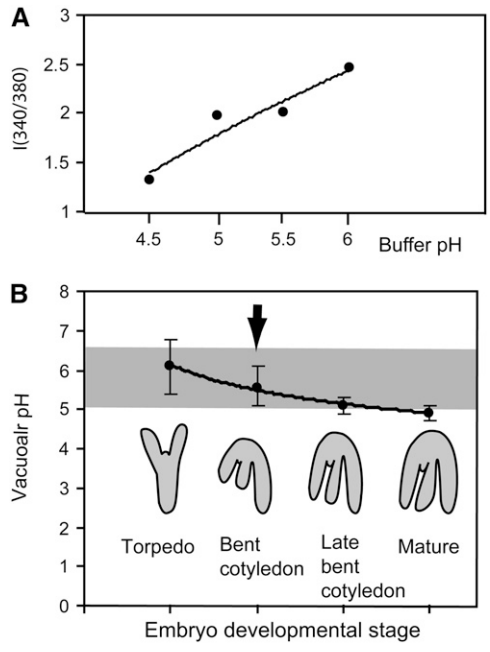


**Figure 9.** Determination of the Luminal pH of PSVs Using Lysosensor Yellow/Blue.

**(A)** Calibration curve.

**(B)** pH inside PSVs during embryo development. The arrow indicates the developmental stage at which storage proteins are first detected inside the PSVs by immunolabeling. The shaded area represents the pH range in which the solubility of the processed 12S globulins is <50%, as reported by Gruis et al. (2004).

## DISCUSSION

We have studied the trafficking of storage proteins, their processing proteases, and the VSR-1/ATELP1 receptor in the *Arabidopsis* embryo during PSV formation. The principal findings of this study are as follows: (1) storage proteins and their processing proteases occupy separate spaces within Golgi cisternae and are packaged into separate vesicles before being delivered to MVBs; (2) the dense vesicles contain both aggregated storage proteins and the VSR-1/ATELP1 receptor; and (3) the proteolytic processing of the 2S albumin storage proteins begins inside the MVBs. A model depicting the trafficking pathways of storage proteins and their processing proteases in *Arabidopsis* embryo cells is shown in Figure 10.

### Storage Proteins and Their Processing Enzymes Are Segregated into Different Cisternal Domains during Golgi Trafficking

Some integral proteins that localize to the PSV, such as the aquaporin α-TIP (Park et al., 2004) and Soybean Gene Regulated by Cold2 (Oufattole et al., 2005), are transported from the ER to the vacuole, bypassing the Golgi, in leaf *Arabidopsis* protoplasts and seeds. However, our results clearly indicate that a Golgi-dependent pathway is responsible for the transport of the soluble seed storage proteins and their processing enzymes to the PSV in *Arabidopsis*.

In *Arabidopsis* embryo cells, the newly synthesized storage proteins are delivered to the *cis*-most Golgi cisterna in a non-aggregated form (Figure 2C). However, upon progressing to the second *cis*-type cisterna, virtually all of the storage proteins become sequestered into dense aggregates that form in the cisternal margins (Figures 2C and 3A to 3H; see Supplemental Figure 1B online). Similar globulin aggregates also form on the *cis* side of Golgi stacks in legume embryo cells (Hillmer et al., 2001; Castelli and Vitale, 2005). Every cisterna, except the first *cis*-cisterna, possesses at least one or two of these protein aggregates, each of which is contained within a cisternal bud (Figure 2C).

The processing proteases were also detected in the Golgi, but they appear to be excluded from the storage protein–containing cisternal buds (Figures 3I, 3J, and 4A). Thus, although the storage proteins and processing proteases share the luminal space of the Golgi cisternae, the access of the processing proteases to the storage proteins is restricted both by the aggregation of the storage proteins and by their segregation into tight-fitting and narrow-necked cisternal buds. Upon reaching either the *trans*-most cisterna or the TGN, these protein aggregate–containing buds give rise to the dense vesicles. Although we do not have direct evidence supporting the notion that β-VPE and the aspartic protease A1 are sorted into the same type of vesicles, based on their occurrence in the same rate-zonal fraction and their immunodetection in the TGN, we hypothesize that they are packaged into clathrin-coated vesicles that become the 30- to 40-nm-diameter uncoated vesicles (Figures 1A and 2B). The two

vesicle types, dense and uncoated, would subsequently fuse to produce the MVBs (Figure 10).

### Receptors That Bind the Storage Proteins May Nucleate Protein Aggregation and Mediate Bud Formation around the Aggregates

The process of protein aggregation appears to play an important role in storage protein sorting in the *Arabidopsis* embryo, but complete targeting of the storage proteins to the PSV also requires a functional VSR-1/ATELP1–type receptor (Shimada et al., 2003a). As documented in Figures 3G and 3H and Supplemental Figure 1D online, the membrane that surrounds the dense vesicles contains the VSR-1 receptor, and these receptor molecules are passed on to the MVBs (Figures 6G to 6I). Interestingly, the VSR-1 receptor also has been postulated to be recycled back from the MVB/prevacuolar compartment to the Golgi/TGN by a retromer-mediated mechanism (Oliviusson et al., 2006). According to our results, in *Arabidopsis* embryo cells, at least some VSR-1 molecules are not recycled from the prevacuolar compartment but are sorted into MVB internal vesicles for degradation in the lumen of the PSV (Figures 4B and 6G to 6I).

In plants, the sorting and trafficking pathways that deliver cargo and membranes to vacuoles vary depending on the species, the tissues, and even the developmental stages of the tissues (Robinson et al., 2005). This natural variability may explain some of the controversies that have arisen around the postulated functions of the VSR/ATELP/BP-80 family of receptors. There is general agreement that these receptors are involved in the sorting of proteins to vacuoles (Ahmed et al., 1997, 2000; Laval et al., 1999; Miller et al., 1999; Li et al., 2002; Paris and Neuhaus, 2002; Shimada et al., 2003a; Happel et al., 2004; Jolliffe et al., 2004). However, because the BP-80 receptor possesses a cytosolic motif for recruiting clathrin coats to vesicles, localizes to such vesicles in legume embryo cells, and sorts proteins such as aleurain to lytic vacuoles (Hinz et al., 1999; Ahmed et al., 2000), most researchers have assumed that the function of these receptors is to sort proteins to lytic vacuoles.

The discovery that the same type of receptor can also mediate the sorting of seed storage proteins to PSVs in pumpkin (*Cucurbita pepo*) (Shimada et al., 2002), *Arabidopsis* (Shimada et al., 2003a), and *Ricinus communis* (Jolliffe et al., 2004) has challenged the assumption that these receptors only serve in the lytic vacuole sorting pathway. The localization of the VSR-1 receptor to the dense vesicle membrane in *Arabidopsis* embryos provides further support for the hypothesis that these receptors can also bind storage proteins. We postulate that the VSR-1 receptors serve two functions in the storage protein trafficking pathway: (1) they could provide the nucleation sites for storage protein aggregation in the cisternal margins; and (2) they could ensure that the membrane surrounding each storage protein aggregate becomes tightly and stably attached to the aggregate and that it produces a narrow neck connection to the cisterna. Both of these features would help limit the access of the processing proteases to the storage proteins.

In contrast with our observations, Hinz et al. (1999) found that the BP-80 receptor was highly enriched in the subcellular fractions from pea cotyledons containing clathrin-coated vesicles and not in the dense vesicle fraction. Why did we not detect the VSR-1 receptor in clathrin-coated vesicles and/or vesicles carrying proteases? One interesting feature of the VSR/ATELP/BP-80 family of receptors is that each species appears to have multiple members. It is very likely that another VSR isoform is responsible for the sorting of proteases into clathrin-coated vesicles. Even if the anti-VSR-1/ATELP1 antibody that we used in this study is able to recognize this other isoform, the density of the receptor in clathrin-coated vesicles from *Arabidopsis* may be too low to be clearly identified by immunodetection in plastic sections or in subcellular fractions. Why did Hinz and colleagues not detect the BP-80 receptor in dense vesicles of pea cotyledons by immunolabeling? Although they detected small amounts of the BP-80 receptor in the subcellular fraction containing dense vesicles, they did not detect BP-80 labeling on dense vesicles in cryosectioned pea embryos. It is important to note that they used a different antibody and a different tissue-processing technique. The anti BP-80 antibody used by Hinz et al. may

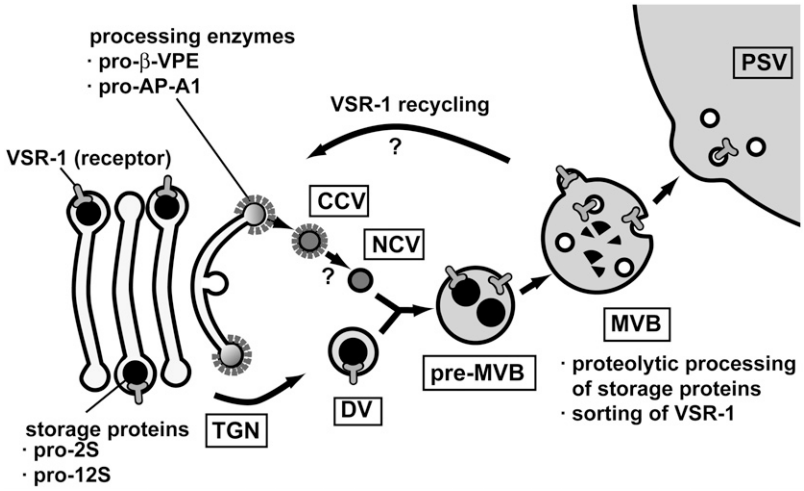


**Figure 10.** Model Depicting the Sorting and Trafficking of Storage Proteins and Processing Proteases in *Arabidopsis* Embryos during PSV Formation.

have a higher affinity for the receptor isoform found in clathrin-coated vesicles than for the receptor of storage proteins. In addition, the different tissue-processing techniques used in their and our studies, chemical fixation/freezing and high-pressure freezing/freeze substitution, respectively, may result in different immunoreactivity preservation.

Another receptor called At RMR1 (for *Arabidopsis* receptor homology region transmembrane domain ring H2 motif protein 1) (Jiang et al., 2000) has been shown to interact in *Arabidopsis* leaf protoplasts with the C-terminal propeptide of the transiently expressed legume 7S globulin phaseolin (Park et al., 2005). Phaseolin is the major storage protein in *Phaseolus vulgaris* seeds. However, *Arabidopsis* seeds accumulate 7S globulins only as a very minor storage protein fraction (R. Jung, unpublished data), and an interaction between a RMR1-like receptor and 2S albumin– and 11S globulin–type storage proteins (the abundant classes of storage proteins in *Arabidopsis* seed) has not been demonstrated.

### MVBs Arise from the Fusion of Dense Vesicles with Small Vesicles

MVBs have been implicated previously in the trafficking of seed storage proteins in legumes (Robinson et al., 1998). However, both the origin and the functions of these MVBs have remained enigmas. Our data indicate that the secretory MVBs in *Arabidopsis* embryos arise from the fusion of dense vesicles with at least one more type of small vesicle, most likely vesicles that deliver the proteases to the MVBs. It is also possible that some of the MVBs enlarge by fusing with each other. The MVBs arise in close proximity to the *trans* side of the Golgi stacks and TGN cisternae (Figure 1A), consistent with the idea that they are produced from freshly budded dense vesicles and small vesicles.

### MVBs Are Sites for the Initial Proteolytic Processing of 2S Albumins

The proteolytic processing of the 2S albumins begins in the MVBs, as shown by the finding that the MVBs contain both unprocessed precursors and processed 2S albumins (Figures 7D to 7F). Although we have not determined the pH inside the MVBs, it is likely that they undergo progressive acidification as they mature. The finding that the VPE Cys and the aspartic protease enzymes are both active inside the MVBs supports the idea of an acidic luminal pH in the MVBs, because the pH optimum for VPEs is pH 5 to 6 and that for the aspartic proteases is pH 3 to 4 (Kuroyanagi et al., 2002). A low pH is also needed for the detachment of ligands from receptors in endosomal/prevacuolar compartments (Kirsch et al., 1994).

At present, we do not know how much of the proteolytic processing of the 2S albumins occurs in the MVBs. The small size of the dense aggregates in the largest MVBs suggests that the removal of the propeptides is largely accomplished in the MVB compartment before the proteins reach the PSVs. Why does this proteolytic processing start in the MVBs and not in the PSVs? As mentioned above, the proteolytic processing of the 2S albumins and 12S globulins requires both VPE Cys proteases and aspartic proteases, which have different pH optima. By activating these enzymes in the MVBs, it is conceivable that the gradual acidification of these MVBs is exploited to process the proteins in a sequential manner, first by activating the VPE Cys proteases and then the aspartic proteases.

Processing of the storage proteins leads to conformational changes that decrease their solubility and make them more resistant to further proteolysis inside the PSVs during seed development (Gruis et al., 2004). In fact, the PSV pH decreases from 5.5 to 4.9 during development (Figure 9), a pH range in which the solubility of the 12S globulins is <50% (Gruis et al., 2004).

### MVBs Function as Prevacuolar Compartments in the Secretory Pathway

MVBs are typically defined as sorting and recycling compartments between early and late endosomes (Geldner, 2004; Gruenberg and Stenmark, 2004). One of their main functions is to invaginate membrane domains containing membrane proteins destined for degradation, a process that gives rise to the characteristic internal vesicles before their transfer to the late endosomes and lysosomes/vacuoles (Katzmann et al., 2002). Whereas most of these membrane proteins are derived from the plasma membrane and therefore correspond to endocytic cargo molecules, it has also been shown that proteins that traffic between the Golgi and lysosomes/vacuoles, such as the mammalian mannose-6-phosphate receptors (Griffiths et al., 1988) and the plant BP-80 receptor (Tse et al., 2004; Oliviusson et al., 2006), can pass through MVBs. In tobacco (*Nicotiana tabacum*) BY2 cells, MVBs appear to traffic VSR-type vacuolar receptors and endocytic markers such as FM4-64, suggesting that the same MVB population is part of both the endocytic and secretory pathways (Tse et al., 2004). However, the diversity of vacuolar compartments in plant cells may also correlate with different kinds of MVB/prevacuolar compartments. In fact, preliminary immunolabeling experiments in *Arabidopsis* embryo cells indicate that protein-containing MVBs do not traffic endocytosed plasma membrane proteins (M.S. Otegui, unpublished data); therefore, they would not be involved in the endocytic pathway. We are currently studying the endocytic trafficking in embryo cells to further explore this hypothesis.

## METHODS

### Antibodies

Peptide antibodies against *Arabidopsis thaliana* 2S precursor 2 N-terminal (SIYRTVVEFDEDDASNPM) and internal (DDEFDLEDDIENPQG) propeptides were raised in rabbits. The antibodies used against *Arabidopsis* β-VPE are described by Gruis et al. (2002). The antibodies against VSR-1/ATELP1 (Ahmed et al., 1997) were bought from Rose Biotechnology, and the monoclonal anti-clathrin heavy chain antibodies were from BD Biosciences Pharmingen. The other antibodies used in this study were requested from the scientific community: antibodies against the *Arabidopsis* 2S albumin large chain were provided by Alessio Scarafoni (University of Milan) (Scarafoni et al., 2001); antibodies against *Arabidopsis* 12S globulins were provided by Ikuko Hara Nishimura (Kyoto University) (Shimada et al., 2003b); anti-α-man (Preuss et al., 2004) and anti-PUX1 antibodies (Rancour et al., 2004) were provided by Sebastian Bednarek (University of Wisconsin-Madison); anti-aspartic protease A1 antibodies were provided by Susannah Gal (State University of New York, Binghamton) (Mutlu et al., 1999); anti-VM23 antibodies were provided by Masayoshi Maeshima (Nagoya University) (Maeshima, 1992); and anti-ACA2 antibodies were provided by Jeffrey F. Harper (Scripps Research Institute) (Hwang et al., 2000).

### Electron Microscopy and Immunolabeling

*Arabidopsis* embryos at different stages of development (torpedo, bent cotyledon, late bent cotyledon, and mature) were high-pressure frozen/freeze substituted for electron microscopy analysis as described previously (Otegui et al., 2002).

For immunolabeling, some high-pressure frozen samples were substituted in 0.2% uranyl acetate (Electron Microscopy Sciences) plus 0.2% glutaraldehyde (Electron Microscopy Sciences) in acetone at −80°C for 72 h and then warmed to −50°C for 24 h. After several acetone rinses, these samples were infiltrated with Lowicryl HM20 (Electron Microscopy Sciences) during 72 h and polymerized at −50°C under UV light for 48 h. Sections were mounted on Formvar-coated nickel grids and blocked for 20 min with a 5% (w/v) solution of nonfat milk in PBS containing 0.1% Tween 20. The sections were incubated in the primary antibodies (1:10 in PBS–Tween 20) for 1 h, rinsed in PBS containing 0.5% Tween 20, and then transferred to the secondary antibody (anti-rabbit IgG, 1:50) conjugated to 15-nm gold particles for 1 h. Controls omitted either the primary antibodies or used the preimmune serum.

Double labeling experiments were performed according to Sanderfoot et al. (1998), with minor modifications. Plastic sections were first blocked with 5% (w/v) milk, then incubated with the first primary antibody followed by incubation in the goat anti-rabbit IgG conjugated to either 15- or 5-nm gold particles, as explained above. After a fixation step (5% glutaraldehyde, 30 min) and a second blocking step with 5% milk, the grids were incubated with either no antiserum or specific antiserum for 1 h, followed by a 1-h incubation with anti-rabbit IgG linked directly to either 5- or 15-nm colloidal gold particles.

For quantification, five independent grids were analyzed, and from each grid, 15 random regions were imaged. Labeling densities of both the N-PP and the 2S albumin antibodies were estimated on Golgi aggregates, free dense vesicles, MVBs, and PSVs by calculating the number of gold particles in standardized $10 \times 10^4$ nm$^2$ areas.

### Electron Tomography

Epon sections (250 nm thick) were mounted on Formvar-coated copper slot grids and stained with 2% uranyl acetate in 70% methanol and Reynold's lead citrate (2.6% lead nitrate and 3.5% sodium citrate, pH 12). Colloidal gold particles (15 nm) were used as fiducial markers to align the series of tilted images. The sections were mounted in a tilt-rotate specimen holder and observed in a FEI Tecnai TF30 intermediate voltage electron microscope (FEI Company) operated at 300 kV. The images were taken at 15,000× from +60° to –60° at 1.0° intervals about two orthogonal axes (Mastronarde, 1997) and collected in a Gatan digital camera at a pixel size of 1.0 nm. The images were aligned as described by Ladinsky et al. (1999). Tomograms were computed for each set of aligned tilts using the R-weighted back-projection algorithm (Gilbert, 1972). Merging of the two single-axis tomograms into a dual-axis tomogram involved a warping procedure (Mastronarde, 1997). Serial tomograms were obtained by combining dual-axis tomograms (Ladinsky et al., 1999). Tomograms were displayed and analyzed with 3Dmod, the graphic component of the IMOD software package (Kremer et al., 1996). Membranous structures and vesicles were modeled as described by Otegui et al. (2001). The thinning factor for each tomogram was calculated and corrected for in the models. The surface area of prevacuolar compartments was calculated using the program Imodinfo of the IMOD software package.

### Analysis of Seed Protein Extracts

SDS-PAGE and immunoblot analyses were performed as described previously (Gruis et al., 2002), with the difference that total protein was extracted from whole seeds in a 20-fold (v/w) excess of 2% SDS, 100 mM DTT, and 50 mM Tris-HCl, pH 6.8, and separated by SDS-PAGE using 10 to 20% gradient Tris-HCl Criterion gels (Bio-Rad).

### Subcellular Fractionation of Vesicles

Secretory vesicles were isolated from late bent-cotyledon *Brassica napus* embryos according to Hinz et al. (1999), with modifications. All procedures were performed at 4°C. Embryos were homogenized in 0.3 M sorbitol, 50 mM MOPS (Sigma-Aldrich)-KOH, pH 6.5, with a protease inhibitor cocktail (Roche). The homogenate was filtered and centrifuged at 200*g* for 10 min. PSVs and other large organelles were isolated by centrifuging the 200*g* supernatant at 2500*g* for 20 min (pellet fraction P2.5). The 2500*g* supernatant was applied onto a 65% sucrose cushion (50 mM MOPS-KOH, pH 6.5) and centrifuged at 16,000*g* for 40 min. The 16,000*g* supernatant was layered onto a sucrose step gradient (20, 35, 42, and 55% [w/v] sucrose in 50 mM MOPS, pH 6.5) and centrifuged at 85,500*g* for 120 min. The 42 to 55% sucrose interphase, which is enriched in secretory vesicles (Hinz et al., 1999), was layered onto a linear sucrose gradient (20 to 55% [w/v] sucrose) and centrifuged at 16,000*g* for 20 min (rate-zonal gradient). Four fractions (fraction 1, 22% sucrose; fraction 2, 25%; fraction 3, 28%; fraction 4, 31%) were collected from the top of the tube. Fractions of interest were normalized to reflect equal amounts of the starting homogenate and analyzed by SDS-PAGE and protein gel blot.

### Ratiometric Estimation of the Intravacuolar pH of PSVs

The pH calibration curve was obtained according to Diwu et al. (1999) and Otegui et al. (2005) with modifications. Embryo cells were isolated by treating small pieces of cotyledons with pectinase (Sigma-Aldrich). These embryo cells were incubated in 20 μM Lysosensor Yellow/Blue DND-160 [2-(4-pyridyl)-5-(4-(2-dimethylaminoethylamino-carbamoyl)-methoxy)-phenyl-oxazole; Molecular Probes) for 1 h. Excess dye was removed by washing the cells with 20 mM MES and 0.45 M betaine buffer, pH 6. For calibration, embryo cells were treated with MES calibration buffers (10 mM MES and 0.45 M betaine), ranging from pH 4.5 to 6.5, and containing 10 μM nigericin (Sigma-Aldrich). Measurements were taken 5 to 10 min after the addition of nigericin. Embryo cells were visualized with an inverted microscope (Nikon Diaphot 200) adapted for epifluorescence and excited at 340 and 380 nm, and the fluorescence emission intensity was recorded at 530 nm. The $I_{340/380}$ was calculated after subtracting the background signal.

To determine the fluorescence emission of PSVs, the $I_{340/380}$ was calculated from embryo cells at different stages of development incubated in 20 μM Lysosensor Yellow/Blue DND-160 with no nigericin added. The fluorescence emission $I_{340/380}$ values obtained from PSVs were converted to absolute values of vacuolar pH by comparison with the calibration curve.

### Accession Numbers

The Arabidopsis Genome Initiative locus identifiers for the genes mentioned in this article are as follows: At3g52850 (VSR-1/ATELP1), At1g11910 (aspartic protease A1), At1g62710 (β-VPE), and At4g27150 (AT2S2).

### Supplemental Data

The following materials are available in the online version of this article.

**Supplemental Figure 1.** Immunolabeling of PSVs, Golgi Stacks, MVBs, and Dense Vesicles in the *Arabidopsis* Embryo.

**Supplemental Figure 2.** Immunolabeling of PSVs in Both Wild-Type and *vpe*-Quadruple Mutant Mature Embryo Cells with the Anti-2S Propeptide Antibodies.

## ACKNOWLEDGMENTS

We thank Sebastian Bednarek (University of Wisconsin, Madison), Susannah Gal (State University of New York, Binghamton), Ikuko

Hara-Nishimura (Kyoto University), Jeffrey F. Harper (Scripps Research Institute), Masayoshi Maeshima (Nagoya University), and Alessio Scarafoni (University of Milan) for the generous gifts of antibodies. We also thank members of the Boulder Laboratory for Three-Dimensional Electron Microscopy of Cells for their support in the electron tomographic analysis, Martin G. Vila Petroff and Alicia Mattiazi (University of La Plata) for the use of the equipment for pH determination, and David Christopher (University of Hawaii) and Matthew Russell (University of Colorado-Boulder) for critical reading of the manuscript. This work was supported by National Institutes of Health Grant GM-61306 to L.A.S., by Grant 14022-14 from the Antorchas Foundation, Argentina, and by funds from the University of Wisconsin, Botany Department, to M.S.O.

Received January 18, 2006; revised July 24, 2006; accepted September 6, 2006; published September 29, 2006.

## REFERENCES

**Ahmed, S.U., Bar-Peled, M., and Raikhel, N.V.** (1997). Cloning and subcellular location of an Arabidopsis receptor-like protein that shares common features with protein-sorting receptors of eukaryotic cells. Plant Physiol. **114,** 325–336.

**Ahmed, S.U., Rojo, E., Kovaleva, V., Venkataraman, S., Dombrowski, J.E., Matsuoka, K., and Raikhel, N.V.** (2000). The plant vacuolar sorting receptor is involved in transport of $NH_2$-terminal propeptide-containing vacuolar proteins in *Arabidopsis thaliana*. J. Cell Biol. **149,** 1335–1344.

**Castelli, S., and Vitale, A.** (2005). The phaseolin vacuolar sorting signal promotes transient, strong membrane association and aggregation of the bean storage protein in transgenic tobacco. J. Exp. Bot. **56,** 1379–1387.

**Chen, X., Pfeil, J.E., and Gal, S.** (2002). The three aspartic proteinase genes of *Arabidopsis thaliana* are differentially expressed. Eur. J. Biochem. **269,** 4675–4684.

**daSilva, L.L.P., Taylor, J.P., Hadlington, J.L., Hanton, S.L., Snowden, C.J., Fox, S.J., Foresti, O., Brandizzi, F., and Denecke, J.** (2005). Receptor salvage from the prevacuolar compartment is essential for efficient vacuolar protein targeting. Plant Cell **17,** 132–148.

**da Silva Conceicao, A., and Krebbers, E.** (1994). A cotyledon regulatory region is responsible for the different spatial expression patterns of *Arabidopsis* 2S albumin genes. Plant J. **5,** 493–505.

**Diwu, Z., Chen, C.-S., Zhang, C., Klaubert, D.H., and Haugland, R.P.** (1999). A novel acidotropic pH indicator and its potential application in labeling acidic organelles of live cells. Chem. Biol. **6,** 411–418.

**Geldner, N.** (2004). The plant endosomal system—its structure and role in signal transduction and plant development. Planta **219,** 547–560.

**Geuze, H.J., Slot, J.W., Strous, G.J.A.M., Lodish, H.F., and Schwartz, A.L.** (1983). Intracellular site of asialoglycoprotein receptor-ligand uncoupling: Double-label immunoelectron microscopy during receptor-mediated endocytosis. Cell **32,** 277–287.

**Gilbert, P.F.C.** (1972). The reconstruction of a three-dimensional structure from projections and its application to electron microscopy. II. Direct methods. Proc. R. Soc. Lond. B Biol. Sci. **182,** 89–102.

**Greenwood, J.S., and Chrispeels, M.J.** (1985). Immunocytochemical localization of phaseolin and phytohemagglutinin in the endoplasmic reticulum and Golgi complex of developing bean cotyledons. Planta **164,** 295–302.

**Griffiths, G., Hoflack, B., Simons, K., Mellman, I., and Kornfeld, S.** (1988). The mannose 6-phosphate receptor and the biogenesis of lysosomes. Cell **52,** 329–341.

**Gruenberg, J., and Stenmark, H.** (2004). The biogenesis of multivesicular bodies. Nat. Rev. Mol. Cell Biol. **5,** 317–323.

**Gruis, D., Schulze, J., and Jung, R.** (2004). Storage protein accumulation in the absence of the vacuolar processing enzyme family of cysteine proteases. Plant Cell **16,** 270–290.

**Gruis, D.F., Selinger, D.A., Curran, J.M., and Jung, R.** (2002). Redundant proteolytic mechanisms process seed storage proteins in the absence of seed-type members of the vacuolar processing enzyme family of cysteine proteases. Plant Cell **14,** 2863–2882.

**Happel, N., Honing, S., Neuhaus, J.-M., Paris, N., Robinson, D.G., and Holstein, S.E.H.** (2004). *Arabidopsis* μA-adaptin interacts with the tyrosine motif of the vacuolar sorting receptor VSR-PS1. Plant J. **37,** 678–693.

**Hillmer, S., Movafeghi, A., Robinson, D.G., and Hinz, G.** (2001). Vacuolar storage proteins are sorted in the *cis*-cisternae of the pea cotyledon Golgi apparatus. J. Cell Biol. **152,** 41–50.

**Hinz, G., Hillmer, S., Bäumer, M., and Hohl, I.** (1999). Vacuolar storage proteins and the putative vacuolar receptor BP-80 exit the Golgi apparatus of developing pea cotyledons in different transport vesicles. Plant Cell **11,** 1509–1524.

**Hohl, I., Robinson, D.G., Chrispeels, M.J., and Hinz, G.** (1996). Transport of storage proteins to the vacuole is mediated by vesicles without a clathrin coat. J. Cell Sci. **109,** 2539–2550.

**Holkeri, H., and Vitale, A.** (2001). Vacuolar sorting determinants within a plant storage protein trimer act cumulatively. Traffic **2,** 737–741.

**Hwang, I., Sze, H., and Harper, J.F.** (2000). A calcium-dependent protein kinase can inhibit a calmodulin-stimulated $Ca^{2+}$ pump (ACA2) located in the endoplasmic reticulum of *Arabidopsis*. Proc. Natl. Acad. Sci. USA **97,** 6224–6229.

**Jiang, L., Phillips, T.E., Hamm, C.A., Drozdowicz, Y.M., Rea, P.A., Maeshima, M., Rogers, S.W., and Rogers, J.C.** (2001). The protein storage vacuole: A unique compound organelle. J. Cell Biol. **155,** 991–1002.

**Jiang, L., Phillips, T.E., Rogers, S.W., and Rogers, J.C.** (2000). Biogenesis of the protein storage vacuole crystalloid. J. Cell Biol. **150,** 755–770.

**Jolliffe, N.A., Brown, J.C., Neumann, U., Vicre, M., Bachi, A., Hawes, C., Ceriotti, A., Roberts, L.M., and Frigerio, L.** (2004). Transport of ricin and 2S albumin precursors to the storage vacuoles of *Ricinus communis* endosperm involves the Golgi and VSR-like receptors. Plant J. **39,** 821–833.

**Katzmann, D.J., Odorizzi, G., and Emr, S.D.** (2002). Receptor down-regulation and multivesicular-body sorting. Nat. Rev. Mol. Cell Biol. **3,** 893–905.

**Kirsch, T., Paris, N., Butler, J., Beevers, L., and Rogers, J.** (1994). Purification and initial characterization of a potential plant vacuolar targeting receptor. Proc. Natl. Acad. Sci. USA **91,** 3403–3407.

**Kremer, J.R., Mastronarde, D.N., and McIntosh, J.R.** (1996). Computer visualization of three-dimensional image data using IMOD. J. Struct. Biol. **116,** 71–76.

**Kuroyanagi, M., Nishimura, M., and Hara-Nishimura, I.** (2002). Activation of *Arabidopsis* vacuolar processing enzyme by self-catalytic removal of an auto-inhibitory domain of the C-terminal propeptide. Plant Cell Physiol. **43,** 143–151.

**Ladinsky, M.S., Mastronarde, D.N., McIntosh, J.R., Howell, K.E., and Staehelin, L.A.** (1999). Golgi structure in three dimensions: Functional insights from the normal rat kidney cell. J. Cell Biol. **144,** 1135–1149.

**Laval, V., Chabannes, M., Carriere, M., Canut, H., Barre, A., Rouge, P., Pont-Lezica, R., and Galaud, J.-P.** (1999). A family of *Arabidopsis* plasma membrane receptors presenting animal β-integrin domains. Biochim. Biophys. Acta **1435,** 61–70.

**Li, Y.-B., Rogers, S.W., Tse, Y.C., Lo, S.W., Sun, S.S.M., Jauh, G.-Y., and Jiang, L.** (2002). BP-80 and homologs are concentrated on post-Golgi, probable lytic prevacuolar compartments. Plant Cell Physiol. **43,** 726–742.

**Maeshima, M.** (1992). Characterization of the major integral protein of vacuolar membrane. Plant Physiol. **98,** 1248–1254.

**Mansfield, S.G., and Briarty, L.G.** (1992). Cotyledon cell development in *Arabidopsis thaliana* during reserve deposition. Can. J. Bot. **70,** 151–164.

**Mastronarde, D.** (1997). Dual-axis tomography: An approach with alignment methods that preserve resolution. J. Struct. Biol. **120,** 343–352.

**Miller, E.A., Lee, M.C.S., and Anderson, M.A.** (1999). Identification and characterization of a prevacuolar compartment in stigmas of *Nicotiana alata*. Plant Cell **11,** 1499–1508.

**Muntz, K.** (1998). Deposition of storage proteins. Plant Mol. Biol. **38,** 77–99.

**Mutlu, A., Chen, X., Reddy, S.M., and Gal, S.** (1999). The aspartic proteinase is expressed in *Arabidopsis thaliana* seeds and localized in the protein bodies. Seed Sci. Res. **9,** 75–84.

**Oliviusson, P., Heinzerling, O., Hillmer, S., Hinz, G., Tse, Y.C., Jiang, L., and Robinson, D.G.** (2006). Plant retromer, localized to the prevacuolar compartment and microvesicles in *Arabidopsis*, may interact with vacuolar sorting receptors. Plant Cell **18,** 1239–1252.

**Otegui, M.S., Capp, R., and Staehelin, L.A.** (2002). Developing seeds of *Arabidopsis* store different minerals in two types of vacuoles and in the endoplasmic reticulum. Plant Cell **14,** 1311–1327.

**Otegui, M.S., Mastronarde, D.N., Kang, B.-H., Bednarek, S.Y., and Staehelin, L.A.** (2001). Three-dimensional analysis of syncytial-type cell plates during endosperm cellularization visualized by high resolution electron tomography. Plant Cell **13,** 2033–2051.

**Otegui, M.S., Noh, Y.S., Martinez, D., Vila Petroff, M., Staehelin, L.A., Amasino, R.M., and Guiamet, J.J.** (2005). Senescence-associated vacuoles with intense proteolytic activity develop in leaves of *Arabidopsis* and soybean. Plant J. **41,** 831–844.

**Oufattole, M., Park, J.H., Poxleitner, M., Jiang, L., and Rogers, J.C.** (2005). Selective membrane protein internalization accompanies movement from the endoplasmic reticulum to the protein storage vacuole pathway in *Arabidopsis*. Plant Cell **17,** 3066–3080.

**Paris, N., and Neuhaus, J.-M.** (2002). BP-80 as a vacuolar sorting receptor. Plant Mol. Biol. **50,** 903–914.

**Paris, N., Stanley, C.M., Jones, R.L., and Rogers, J.C.** (1996). Plant cells contain two functionally distinct vacuolar compartments. Cell **85,** 563–572.

**Park, M., Kim, S.J., Vitale, A., and Hwang, I.** (2004). Identification of the protein storage vacuole and protein targeting to the vacuole in leaf cells of three plant species. Plant Physiol. **134,** 625–639.

**Park, M., Lee, D., Lee, G.-J., and Hwang, I.** (2005). AtRMR1 functions as a cargo receptor for protein trafficking to the protein storage vacuole. J. Cell Biol. **170,** 757–767.

**Preuss, M.L., Serna, J., Falbel, T.G., Bednarek, S.Y., and Nielsen, E.** (2004). The *Arabidopsis* Rab GTPase RabA4b localizes to the tips of growing root hair cells. Plant Cell **16,** 1589–1603.

**Rancour, D.M., Park, S., Knight, S.D., and Bednarek, S.Y.** (2004). Plant UBX domain-containing protein 1, PUX1, regulates the oligomeric structure and activity of *Arabidopsis* CDC48. J. Biol. Chem. **279,** 54264–54274.

**Robinson, D.G., and Hinz, G.** (1999). Golgi-mediated transport of seed storage proteins. Seed Sci. Res. **9,** 267–283.

**Robinson, D.G., Baeumer, M., Hinz, G., and Hohl, I.** (1998). Vesicle transfer of storage proteins to the vacuole: The role of the Golgi apparatus and multivesicular bodies. J. Plant Physiol. **152,** 659–666.

**Robinson, D.G., Oliviusson, P., and Hinz, G.** (2005). Protein sorting to the storage vacuoles of plants: A critical appraisal. Traffic **6,** 615–625.

**Sanderfoot, A.A., Ahmed, S.U., Marty-Mazars, D., Rapoport, I., Kirchhausen, T., Marty, F., and Raikhel, N.V.** (1998). A putative vacuolar cargo receptor partially colocalizes with AtPEP12p on a prevacuolar compartment in *Arabidopsis* roots. Proc. Natl. Acad. Sci. USA **95,** 9920–9925.

**Scarafoni, A., Carzaniga, R., Harris, N., and Croy, R.** (2001). Manipulation of the napin primary structure alters its packaging and deposition in transgenic tobacco (*Nicotiana tabacum* L.) seeds. Plant Mol. Biol. **46,** 727–739.

**Shimada, T., Fuji, K., Tamura, K., Kondo, M., Nishimura, M., and Hara-Nishimura, I.** (2003a). Vacuolar sorting receptor for seed storage proteins in *Arabidopsis thaliana*. Proc. Natl. Acad. Sci. USA **100,** 16095–16100.

**Shimada, T., Watanabe, E., Tamura, K., Hayashi, Y., Nishimura, M., and Hara-Nishimura, I.** (2002). A vacuolar sorting receptor PV72 on the membrane of vesicles that accumulate precursors of seed storage proteins (PAC vesicles). Plant Cell Physiol. **43,** 1086–1095.

**Shimada, T., et al.** (2003b). Vacuolar processing enzymes are essential for proper processing of seed storage proteins in *Arabidopsis thaliana*. J. Biol. Chem. **278,** 32292–32299.

**Staehelin, L.A., Giddings, T.H., Kiss, J.Z., and Sack, F.D.** (1990). Macromolecular differentiation of Golgi stacks in root tips of *Arabidopsis* and *Nicotiana* seedlings as visualized in high pressure frozen and freeze-substituted samples. Protoplasma **157,** 75–91.

**Swanson, S.J., Bethke, P.C., and Jones, R.L.** (1998). Barley aleurone cells contain two types of vacuoles: Characterization of lytic organelles by use of fluorescent probes. Plant Cell **10,** 685–698.

**Tse, Y.C., Mo, B., Hillmer, S., Zhao, M., Lo, S.W., Robinson, D.G., and Jiang, L.** (2004). Identification of multivesicular bodies as prevacuolar compartments in *Nicotiana tabacum* BY-2 cells. Plant Cell **16,** 672–693.

**Vitale, A., and Hinz, G.** (2005). Sorting of proteins to storage vacuoles: How many mechanisms? Trends Plant Sci. **10,** 316–323.

**Wenzel, D., Schauermann, G., von Lupke, A., and Hinz, G.** (2005). The cargo in vacuolar storage protein transport vesicles is stratified. Traffic **6,** 45–55.